



# Glass microspheres strengthened magnetorheological plastomers for sound insulation



Chuanlin Sun, Haoming Pang, Shouhu Xuan\*, Xinglong Gong\*

CAS Key Laboratory of Mechanical Behavior and Design of Materials, Department of Modern Mechanics, CAS Center for Excellence in Complex System Mechanics, University of Science and Technology of China, Hefei, Anhui 230027, China

## ARTICLE INFO

### Article history:

Received 26 April 2019

Received in revised form 17 July 2019

Accepted 31 August 2019

Available online 3 September 2019

### Keywords:

Magnetorheological

Glass microsphere

Composite

Sound insulation

## ABSTRACT

The magnetorheological plastomers strengthened by glass microspheres (GMRPs) were prepared for acoustic materials with controllable properties and both the rheological properties and sound insulation characteristics were investigated. The addition of glass microspheres can improve the sound insulation at the whole frequency range. The increasing mass fraction of carbonyl iron powders and the magnetic field significantly affected the sound insulation at first resonance frequency. Finally, a vibration transfer method was established to predict the sound attenuation properties based on the mechanical properties and the fitting curve matched the experimental results very well.

© 2019 Elsevier B.V. All rights reserved.

## 1. Introduction

Acoustic materials attract increasing attention for solving the noise problem in our daily life. Traditional acoustic materials are generally fibrous, perforated or membranous. During the past decade, various new types acoustic materials such as foam composites [1–3] and fibrous metals [4,5], have been constantly investigated and they exhibited excellent acoustic properties. However, the acoustic properties are un-tunable once the materials are prepared, which usually limits their practical application. Magnetorheological (MR) materials have been widely applied in vibration control because of magnetic field dependent mechanical properties [6,7]. Most of the previous works were focused on investigating the magnetorheological mechanism and applications to vibration control [8,9]. The researches indicated that the microstructure in the MR materials were adjustable by applying the external magnetic field. It was found that the controllable mechanical properties have significant influence on the acoustic properties. Combining traditional acoustic materials with the MR materials provides a new approach to control the noise precisely. Because of tunable mechanical behavior, the magnetorheological elastomers (MREs) and magnetorheological fluids (MRFs) were considered as actively sound barriers or acoustic metamaterial [10,11]. However, the MRF is easy to be precipitated [12] and the MRE shows a small MR effect [13]. Therefore, in consideration of their unique MR effects, developing

high performance MR materials for practical acoustic application is of special importance.

Herein, the glass microsphere was chosen to strengthen the MRPs toward good acoustic characteristics. The rheological properties and sound insulation characteristics of the GMRPs were investigated. At the same time, a vibration transfer model was built to establish the relationship between the modulus and the sound insulation.

## 2. Experiments

The samples were prepared by mixing the polyurethane matrix with additives, including carbonyl iron powders (CIPs, type CN, 6.0  $\mu\text{m}$ , BASF AG, Germany) and glass microspheres (GMs, 150  $\mu\text{m}$ , Langfang Nuosen glass products Co. Ltd, China). The polyurethane matrix was fabricated with toluene diisocyanate (TDI, 2,4-TDI at B80%, 2,6-TDI at B20%, Tokyo Chemical Industry Co. Ltd, Japan) and polypropylene glycol (PPG-1000, Sinopec Group Co. Ltd, China). The samples with different mass fractions of CIPs and GMs were prepared (see Section 1 in the Supplementary data).

The mechanical properties of GMRPs under low shear rate were measured by a plate-plate magneto-rheometer (Physica MCR 302, Anton Paar Co., Austria). The samples were 1 mm in thickness, 20 mm in diameter and set between the rotor and the substratum of the rheometer. The magnetic flux density ranged from 0 mT to 960 mT. The magnetic field sweeping tests were carried out with a parallel plate under the shear rate and amplitude of 1 Hz and 0.1% at room temperature.

\* Corresponding authors.

E-mail addresses: [xuansh@ustc.edu.cn](mailto:xuansh@ustc.edu.cn) (S. Xuan), [gongxl@ustc.edu.cn](mailto:gongxl@ustc.edu.cn) (X. Gong).

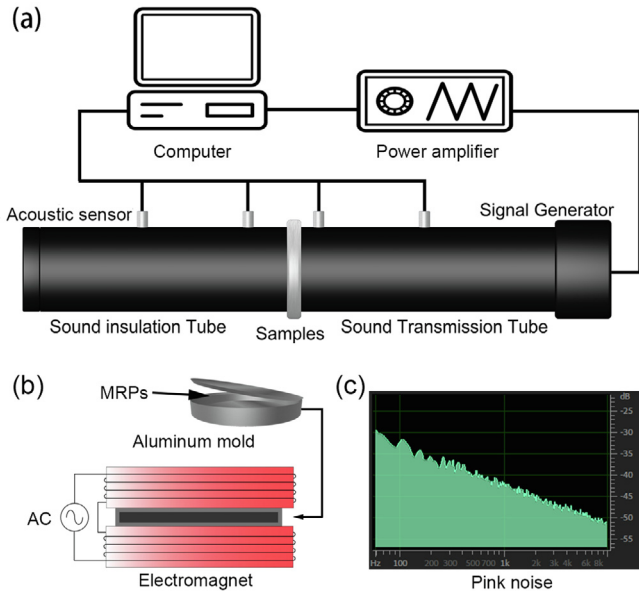


**Fig. 1.** The scheme of the acoustic test system (a), the aluminum mold in the magnetic field (b) and frequency spectrum of pink noise (c). (For interpretation of the references to colour in this figure legend, the reader is referred to the web version of this article.)

The acoustic performance was carried out by an acoustic test system (Fig. 1a). The samples were encapsulated in an aluminum mold and the mold was designed to be 10 mm in thickness and 100 mm in diameter. The sound waves used in experimental tests were pink noise (Fig. 1c), which was one of the most commonly used acoustic waves in acoustic tests.

### 3. Results and discussion

The SEM images showed the surface topography of the material (Fig. 2a) and the chain microstructure under the external magnetic field (Fig. 2b). The magnetic field sweeping tests were conducted to investigate the modulus of GMRPs with different mass fractions of GMs and CIPs (Fig. 2c, d). Obviously, with increasing the magnetic field density, the  $G'$  and  $G''$  increased rapidly at first and became

stabilized gradually. The initial storage modulus ( $G'_0$ ) was highly dependent on the content of GMs. Differently, the samples with higher mass fractions of CIPs performed stronger saturated storage modulus. When the magnetic field density was weak, the magnetic induced modulus of GMRPs was small and the  $G'$  was mainly provided by the glass microspheres. However, when the magnetic field density was strong, the CIPs in the GMRPs were arranged in chains (Fig. 2b). Then the  $G'$  was mainly influenced by magnetic induced modulus.

The acoustic characteristics were studied by an acoustic test system. Fig. 2(e)–(h) depicted the typical sound attenuation curves of the sandwich structure made up by the GMRPs and the mold at low frequencies. The typical sound attenuation curves perform a dramatic drop and this frequency range was called the first resonance frequency. The glass microspheres can effectively improve the sound insulation performance and the sound attenuation volume of the sample with 20% GMs was significantly higher than that of the sample without GMs (Fig. 2f).

The mass fraction of CIPs and the magnetic field intensity only affected the first resonance frequency and they had little influence on the other frequency range. With increasing the mass fraction of CIPs, the first resonance frequency moved to higher frequency and the sound attenuation volume at the first resonance frequency decreased (Fig. 2e). The magnetic field can increase the first resonance frequency and the sound attenuation volume at the first resonance frequency (Fig. 2g, h).

In order to well understand the sound insulation of GMRPs, a model based on vibration transfer was developed. We investigated the transmission of sound indirectly through analyzing the vibration transfer. When the sound arrived at the surface of the mold, the mold was excited. After the vibration passed through the mold and the sample, the other side of the mold vibrated to produce a new sound field. The sound field generated by vibration of a circular plate can be expressed as (Fig. 3a):

$$p = 2\rho_0 c_0 u_0 \sin \frac{k}{2}(R-z) e^{i(\omega t - (\frac{k}{2})(R+z) + \pi/2)} \quad (1)$$

where  $p$  is the sound pressure on the circular normal axis,  $\rho_0$  is the air density,  $c_0$  is the sound speed in air,  $u_0$  is the velocity amplitude of the mold surface,  $k$  is the wave vector.

Considering the actual parameters,  $k = \omega/c_0 < 1$  and  $a = 0.05$ , we can draw a conclusion that  $k(R-z) < ka \ll 1$ . Then, the expression of  $p$  can be simplified as:

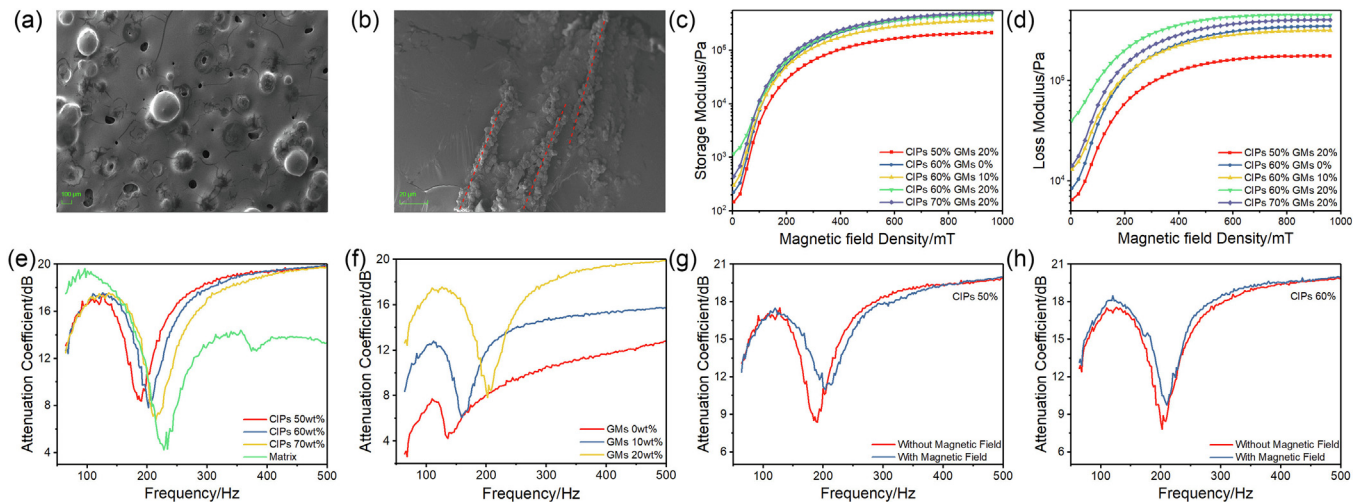


**Fig. 2.** The SEM images and characterizations of GMRPs the samples: the SEM images of samples (a), (b), the storage and loss modulus of GMRPs (c), (d) and the sound insulation influenced by the components and magnetic field (e)–(h).

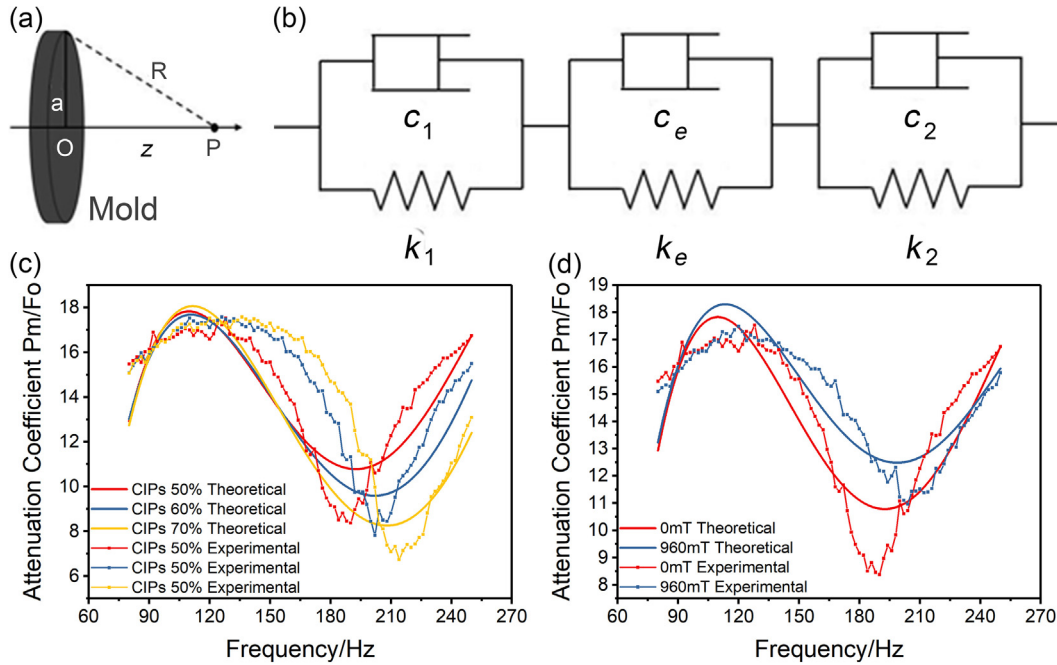


**Fig. 3.** Schematic diagram of each parameter in the formula (a) and the two-element model used for representing the viscoelasticity interface (b) and the comparison of experimental results and theoretical analysis of samples with 20% GMs (c), (d).

$$p = a\rho_0 u_0 \omega e^{i(\omega t - (\frac{\pi}{2})(R+z) + \pi/2)} \quad (2)$$

The displacements of two sides of the mold,  $x_1$  and  $x_2$  are set to be  $x_1 = A_1 e^{i\omega t}$  and  $x_2 = A_2 e^{i\omega t}$ . The sound pressure  $p$  can be further simplified to be:

$$p = a\rho_0 \omega^2 |A_2| e^{i(\omega t - (\frac{\pi}{2})(R+z) + \pi/2)} = p_m e^{i(\omega t - (\frac{\pi}{2})(R+z) + \pi/2)} \quad (3)$$

The coefficient of the expression is the sound pressure amplitude  $p_m = a\rho_0 \omega^2 |A_2|$ . As a sine excitation,  $F$  is set to be  $F_0 e^{i\omega t}$  and  $F_0$  is the amplitude of the incentive force. According to the definition of the transmission loss (Section 2 in the Supplementary data), we can derive its expression:

$$TL = 20 \lg \left( \frac{p_i}{p_t} \right) = 20 \lg \left( \frac{\pi \rho_0 \omega^2 a^3 |A_2|}{F_0} \right) \quad (4)$$

Assume that the GMRPs are always in close contact with the mold wall and their elastic coefficient and viscous coefficient are  $k_e$  and  $c_e$ . The sound come from the right side of the mold provided an incentive force  $F$  to the mold through the vibrating air. According to the model in the Fig. 3b, the equation can be expressed as follows:

$$\begin{cases} m_0 \ddot{x}_1 + k_1 x_1 + k_e (x_1 - x_2) + c_1 \dot{x}_1 + c_e (\dot{x}_1 - \dot{x}_2) = F_0 e^{i\omega t} \\ m_0 \ddot{x}_2 + k_2 x_2 + k_e (x_2 - x_1) + c_2 \dot{x}_2 + c_e (\dot{x}_2 - \dot{x}_1) = 0 \end{cases} \quad (5)$$

where  $m_0$  is the mass of the aluminum layer. We can derive the expression of  $A_2$  by solving the equation:

$$\frac{A_2}{F_0} = \left[ (k_2 + i\omega c_2 - m_0 \omega^2) + \frac{(k_2 + k_e - m_0 \omega^2 + i\omega c_2 + i\omega c_e)(k_1 - m_0 \omega^2 + i\omega c_1)}{k_e + i\omega c_e} \right]^{-1} \quad (6)$$

In this expression, the elastic coefficient and viscous coefficient of columnar samples can be approximately expressed as a simple function of the storage modulus and loss modulus as follows:

$$k_e = \pi G' r^2 / d \quad (7)$$

$$c_e = \pi G'' r^2 / (\omega d) \quad (8)$$

Fig. 3(c, d) shows the calculation results and the trend of the fitting curve matches the experimental result very well. Therefore, this vibration transfer model is competent to predict the sound insulation characteristics of GMRPs.

The sandwich structure had its inherent frequency. Resonance occurred when the acoustic frequency and the inherent frequency converged. At the resonance frequency, a large amount of sound energy was converted into kinetic energy and most sound waves penetrated through the samples which decreased the sound insulation. Therefore, the sound attenuation curves performed a dramatic drop at around 200 Hz. The inherent frequency was usually proportional to the square root of the ratio of the elastic coefficient to the mass, which can be expressed as follows:

$$\omega_n \propto \sqrt{\frac{k}{m}} \quad (9)$$

With the increasing magnetic field, CIPs in the matrix were rearranged into a chain structure. Thus, the  $G'$  increased dramatically which augmented the elastic coefficient. As a result, the inherent frequency moved to the high frequency part. The  $G''$  also increased with magnetic field which augmented the viscous resistance of the materials. More sound energy was consumed during sonic transmission and then the sound attenuation properties were improved (Section 3 in the Supplementary data).

#### 4. Conclusions

In this work, glass microspheres strengthened magnetorheological plastomers were developed to improve the sound attenuation properties of the MRPs. Both the mass fractions of CIPs and glass microspheres affected the mechanical properties and adjusted the sound insulation properties of magnetorheological plastomers. Under applying the magnetic field, the GMRPs show tunable attenuation frequencies, thus they are able to replace traditional sound

insulation materials where the active control is needed. A vibration analysis model was developed to predicting the sound attenuation properties and the theoretical results matched the experimental results well. Therefore, the GMRPs possess broad potential in acoustic materials with active controllability.

#### Declaration of Competing Interest

The authors declare that they have no known competing financial interests or personal relationships that could have appeared to influence the work reported in this paper.

#### Acknowledgements

The financial supports from the National Natural Science Foundation of China (Grant No. 11572309, 11822209) and the Strategic Priority Research Program of the Chinese Academy of Sciences (Grant No. XDB22040502) are gratefully acknowledged. This study was also supported by the Collaborative Innovation Center of Suzhou Nano Science and Technology.

#### Appendix A. Supplementary data

Supplementary data to this article can be found online at <https://doi.org/10.1016/j.matlet.2019.126611>.

#### References

- [1] M. Álvarez-Láinez, M.A. Rodríguez-Pérez, J.A. de Saja, *Mater. Lett.* 121 (2014) 26–30.
- [2] C. Gaulon, J. Pierre, C. Derec, L. Jaouen, F.-X. Bécot, F. Chevillotte, F. Elias, W. Drenckhan, V. Leroy, *Appl. Phys. Lett.* 112 (26) (2018) 261904.
- [3] Y. Xu, Y. Li, A. Zhang, J. Bao, *Mater. Lett.* 194 (2017) 234–237.
- [4] H. Meng, Q.B. Ao, S.W. Ren, F.X. Xin, H.P. Tang, T.J. Lu, *Compos. Sci. Technol.* 107 (2015) 10–17.
- [5] X. Tang, Y. Xiong, *Compos. A Appl. Sci. Manuf.* 101 (2017) 360–380.
- [6] G. Liao, Y. Xu, F. Wang, F. Wei, Q. Wan, *Mater. Lett.* 174 (2016) 79–81.
- [7] J. Yang, H. Yan, X. Wang, Z. Hu, *Mater. Lett.* 167 (2016) 27–29.
- [8] T. Hu, S. Xuan, L. Ding, X. Gong, *Mater. Des.* 156 (2018) 528–537.
- [9] S. Sun, J. Yang, W. Li, H. Deng, H. Du, G. Alici, T. Yan, *Smart Mater. Struct.* 25 (5) (2016) 055035.
- [10] A.R. Baev, E.V. Korobko, Z.A. Novikova, *J. Intell. Mater. Syst. Struct.* 26 (14) (2015) 1913–1919.
- [11] S. Xiao, G. Ma, Y. Li, Z. Yang, P. Sheng, *Appl. Phys. Lett.* 106 (9) (2015) 091904.
- [12] J.D. Vicente, D.J. Klingenberg, R. Hidalgo-Alvarez, *Soft Matter* 7 (8) (2011) 3701–3710.
- [13] C.J. Lee, S.H. Kwon, H.J. Choi, K.H. Chung, J.H. Jung, *Colloid Polym. Sci.* 296 (9) (2018) 1609–1613.